ELSEVIER

Contents lists available at ScienceDirect

# Journal of Membrane Science

journal homepage: www.elsevier.com/locate/memsci



# A novel monoamine modification strategy toward high-performance organic solvent nanofiltration (OSN) membrane for sustainable molecular separations



Yan Chao Xu, Xi Quan Cheng, Jun Long, Lu Shao\*

School of Chemical Engineering and Technology, State Key Laboratory of Urban Water Resource and Environment (SKLUWRE), Harbin Institute of Technology, Harbin 150001, PR China

# ARTICLE INFO

Article history:
Received 12 June 2015
Received in revised form
31 August 2015
Accepted 14 September 2015
Available online 16 September 2015

Keywords:
Organic solvent nanofiltration (OSN)
Monoamine modification
Tris(hydroxymethyl) aminomethane
Membrane-solvent mutual affinity
Solvent permeance

#### ABSTRACT

The main drawback of polyimide (PI) based OSN membrane capable to separate molecules is the declined solvent permeance after crosslinking. In this study, the hydrophilic monoamine named as Tris(hydroxymethyl) aminomethane (Tris) was first utilized to modify polyimide OSN membranes by adding Tris into the dope solution before phase inversion and diamino crosslinking for improving membrane-solvent mutual affinity so as to obtain high-performance OSN membranes. Such Tris modified membranes were proved by chemical characterizations, and the further contact angles and surface energy measurements revealed that the hydrophilicity and surface energy of the novel membranes increased with the Tris loading. Interestingly, the morphological observation demonstrated that the macrovoids shown in the pristine membranes can be completely displaced by sponge-like pores in Tris modified membranes. Surprisingly, the isopropanol (IPA) permeance of 10% Tris modified crosslinked membranes increased to 270% of the original value with only slight decline in dyes rejections. Besides, the fundamental study on the relationship between IPA or N,N-dimethylformamide (DMF) permeance and the membrane-solvent solubility parameter distance were performed. Our novel monoamine modification strategy can provide a new incentive to develop advanced membranes applicable to aqueous solution separation, gas separation and pervaporation for future sustainable usages.

© 2015 Elsevier B.V. All rights reserved.

# 1. Introduction

Organic solvent nanofiltration (OSN) is an emerging and burgeoning technology that can separate molecules in the range from 200 to 2000 g mol<sup>-1</sup> in solvent streams, realizing "green" separation driven by the less energy consumption without any secondary contamination [1–5]. Basically, OSN is a pressure driven membrane separation process depending on the molecular (size, shape and/or charge) diversity. Currently, the most commonly used OSN membranes are integrally skinned asymmetric (ISA) polymeric membranes. Such membranes can be prepared directly by phase inversion *via* immersion precipitation [6], which has the advantages of simplicity to scale-up and low manufacturing cost.

Abbreviations: OSN, organic solvent nanofiltration; Tris, Tris(hydroxymethyl) aminomethane; IPA, isopropanol; DMF, N,N-dimethylformamide; ISA, integrally skinned asymmetric; PDMS, polydimethylsiloxane; Pl, polyimide; HDA, 1,6-hexanediamine; RB, Rose Bengal; MO, Methyl Orange; FT-IR, Fourier transform infrared; XPS, X-ray photoelectron spectroscopy; SE, surface energy; SEM, scanning electron microscope

Regarding to the membrane structure, the typical ISA membrane possesses a skin-layer on the top of a porous and either finger-like or sponge-like support layer with the same chemical composition. Both the inherent material properties and the skin-layer structure determining the selectivity and permeance are critical for manipulating ISA membrane performance.

Up to now, the polyimide resistant to polar aprotic solvents is one of the most attractive materials to prepare ISA OSN membrane for sustainable applications [7–10]. The diamine-induced crosslinking, *via* the reaction between amine groups of diamine and imide groups of polyimide, is the most preferred approach to achieve better separation performance of polyimide membrane due to the easy operation and high efficiency [11]. Shao et al. have investigated the mechanism of diamino crosslinking reaction between various diamines and polyimides [12–14]. They indicated that the reactivity of diamino crosslinking can be greatly influenced by the molecular lengths and nucleophilicity of crosslinking reagents. Diamines with the shorter molecular length and stronger nucleophilicity are much preferred for such crosslinking reaction.

Although the diamino crosslinking approach renders the membrane stability in polar aprotic solvent, it also results in the significant loss of solvent permeance due to a great reduction in

Corresponding author. Fax: +86 451 86418270. E-mail addresses: shaolu@hit.edu.cn, odysseynus@hotmail.com (L. Shao).

interstitial spaces among polymer chains through the inclusion of covalent crosslinkers into the polymer matrix [7]. Therefore, both maintaining the stability of membranes in harsh solvent environment and enhancing the solvent permeance are critically important for high-performance OSN membranes. Unlike in aqueous solution, the interactions between solvent and OSN membrane are much more complicated [15-24]. Different types of solvents may interact with a same membrane in an extremely dissimilar way. For example, a membrane having a high permeance in one solvent may demonstrate a low permeance in another solvent. Interestingly, literatures emphasizing on the relationship between membrane-solvent interactions and solvent permeance in ISA OSN polyimide membrane is still rarely. See-Toh et al. have reported that a P84 polyimide membrane crosslinked with 1,8-octanediamine had a higher toluene permeance compared to methanol. However, the opposite trend in a similar noncrosslinked membrane can be found [7]. They explained that 1,8octanediamine increased the hydrophobicity of the diamino crosslinked membrane, resulting in a higher toluene permeance. Siddique et al. have used Jeffamine 400 and diamine terminated polydimethylsiloxane (PDMS) to chemically crosslink P84 polyimide membranes for investigating the separation performance of crosslinked membranes in acetone and toluene [25]. They have found that such hydrophilic crosslinked membranes show a higher permeance for polar acetone than that of non-polar toluene. However, the long chain length of diamine terminated PDMS has limited its diffusion coefficient in membrane, and a cross-linking time up to 5 days must be needed. Besides, the resulting crosslinked membrane lost nearly 6% weight in DMF due to a low crosslinking degree, indicating the declined membrane stability.

In addition, the incorporation of hydrophilic nanoparticles into a polyimide OSN membrane can influence solvent permeance. Iwona Soroko et al. have prepared a TiO<sub>2</sub>/P84 composite OSN membrane by adding TiO<sub>2</sub> nanoparticles into polyimide dope solution before phase inversion and crosslinking [26]. Such composite membrane showed an enhanced ethanol permeance, meanwhile a declined DMF permeance compared to TiO<sub>2</sub>-free membrane. They ascribed the enhanced ethanol permeance to the increased hydrophilicity of membrane. However, no further explanation on the different trend between ethanol and DMF permeance has been provided.

Besides various diamines, triamines [27,28], multiamine [29,30] and polyamines [28] have been used to prepare cross-linked polyimide OSN membrane. However, as the best of our knowledge, the incorporation of the monoamine in the crosslinked polyimide membrane has not been reported yet. Tris (hydroxymethyl) aminomethane (Tris) is an organic compound commonly used for preparing buffer solutions with one amine group and three hydroxyl groups in one Tris molecular. The amine group of Tris can be utilized to chemically react with polyimide, while the hydroxyl groups could improve the hydrophilicity of modified polyimide membrane. So we are intrigued if the linear polyimide main chains can be partially grafted with Tris for hydrophilic modification before diamino crosslinking, which should endow the membrane with both stability and improved hydrophilicity to greatly enhance the membrane performance.

Herein, we first prepared the novel OSN membranes by grafting hydrophilic Tris monoamines onto P84 polyimide. By adding Tris into the dope solution before phase inversion and diamino crosslinking, the grafting degree can be precisely controlled. The ratio of Tris to imide groups in polyimide and the solvent ratio of DMF to dioxane in the dope solution have been carefully investigated for obtaining the best performance. The physicochemical properties of OSN membrane before and after Tris modification have been examined in detail. The improved hydrophilicity of the Tris modified membrane has been studied, which may lead to

high IPA permeance. The mutual affinity between solvent and membrane material has been analyzed. The outcomes of the study may provide insightful guidelines for developing advanced separating membranes for sustainable applications.

#### 2. Materials and methods

# 2.1. Materials

P84 polyimide was purchased from HP Polymer Gmbh (Austria). N,N-dimethylformamide (DMF), 1,4-dioxane (dioxane) and isopropanol (IPA) were purchased from Xilong Chemical Industrial Co., Ltd. Tris, 1,6-hexanediamine (HDA), Rose Bengal (RB) and Methyl Orange (MO) were obtained from Aladdin Industrial Co., Ltd. PEG200 and PEG400 was purchased from Sinopharm Chemical Reagent Co., Ltd. All used water was deionized.

# 2.2. Membrane preparation

Integrally skinned asymmetric polyimide membranes were prepared via the phase-inversion process. The P84 polyimide polymer was first dried in a vacuum oven at 80 °C overnight to remove moisture before usage. During the preparation of dope solutions, DMF was used as the solvent and dioxane was used as the co-solvent. PI was dissolved at different polymer concentrations with varying DMF:dioxane ratios and the solution was stirred until polymer completely dissolved. Then, the stipulated Tris was added into the solution. The dope solutions were heated to 75 °C for 12 h, and then degassed for a further 12 h at 75 °C to eliminate any air bubble trapped in the solutions. After cooled to room temperature, the dope solutions were cast on a glass plate by using a casting knife with a fixed thickness of 200 µm. Solvent was allowed to evaporate from the surface of the film for 10 s before parallel immersion into a precipitation water bath at room temperature.

All membranes were washed with distilled water for 3 h to remove any residual solvent, and then immersed into a bath of IPA for another 3 h to remove water. In the next step, the membranes were transferred from IPA to the crosslinking solution (2 wt% HDA in IPA) for 24 h. After that, the crosslinked membranes were rinsed with IPA to remove any residual HDA. Finally, the crosslinked membranes were subjected to a conditioning step in which they were kept overnight in a conditioning solution comprised of PEG400/IPA (60/40 wt%). Pieces of membranes used for Fourier transform infrared spectroscopy, X-ray photoelectron spectroscopy, gel content determination and contact angle tests were not subjected to the conditioning step. Finally, the membranes were then air dried to remove resident solvent.

The weight of stipulated Tris,  $w_t$ , was determined using the following equation:

$$w_{\rm t} = \frac{w_{\rm p}}{M_{\rm p}} \times 2 \times M_{\rm t} \times x \tag{1}$$

where  $w_p$  is the weight of P84 in dope solution,  $M_p$  is the molar weight of one repeat unit in P84 (410 g mol<sup>-1</sup>) [10],  $M_t$  is the molar weight of Tris (121 g mol<sup>-1</sup>) and x is the molar ratio of Tris to imide in P84. The membrane preparation conditions are summarized in Table 1, and the membrane fabrication protocol and possible reaction mechanism are shown in Fig. 1.

#### 2.3. Membrane characterization

Fourier transform infrared (FT-IR) was performed on a Spectrum One FT-IR spectrometer (Perkin-Elmer, USA). ZnSe was used

**Table 1** Membrane preparation conditions.

Membrane	P84 wt%	DMF:dioxane	Tris:Imide (%)
M1	22	2:1	0
M2	22	2:1	5
M3	22	2:1	7.5
M4	22	2:1	10
M5	22	2:1	12.5
M6	22	2:1	15
M7	22	2:1	20
M8	22	3:1	0
M9	22	3:1	10
M10	22	1:1	0
M11	22	1:1	10
M12	20	2:1	0
M13	20	2:1	10
M14	24	2:1	0
M15	24	2:1	10

as the crystal plate and all spectra were recorded over the wave number range from 4000 to  $1000\,\mathrm{cm^{-1}}$ . X-ray photoelectron spectroscopy (XPS) experiments were carried out on an AXIS ULTRA DLD spectrometer (SHIMADZU, Japan) using a monochromatized Al K $\alpha$  X-ray source (1486.6 eV photons) at a constant dwell time of 250 ms and a pass energy of 20 eV. A contact angle measuring system (G10 Kruss, Germany) was used to measure the static water contact angle between the water and membranes. Deionized water and diiodomethane were utilized to evaluate the surface energy (SE). The reported contact angle was calculated by averaging over more than five contact angle values at different sites. SE is the sum of polar and disperse parts. SE and its components are calculated by Eq. (2):

$$\gamma_{1}(1 + \cos \theta) = \frac{4\gamma_{s}^{d}\gamma_{1}^{d}}{\gamma_{s}^{d} + \gamma_{1}^{d}} + \frac{4\gamma_{s}^{p}\gamma_{1}^{p}}{\gamma_{s}^{p} + \gamma_{1}^{p}}$$
(2)

where  $\gamma$  refers to surface energy, the subscript 1 and s refer to

liquid and solid, and the superscripts d and p refer to dispersive and polar components, respectively.  $\theta$  refers to contact angles between ordinary liquids (H2O or diiodomethane) and the substrates. Viscosity of dope solutions were investigated using a NDJ-8S viscometer (Scientific Instrument of Shanghai, China) at 20 °C at the rotational speed of 6 rpm with 3 spindle. Images of crosssectional areas of the membranes were obtained using SEM (SEM Quanta 200F, FEI Company). The membranes were fractured in liquid nitrogen to avoid destroying the pore structures of the membranes, mounted onto SEM stubs, and coated with gold layer. The membrane porosity was characterized by PEG uptake [31]. Two disks samples of equal sizes were cut from a membrane and the thicknesses were measured. One was dried in the oven, and the other one was dipped into a PEG200/IPA or PEG400/IPA (60/ 40 wt%) solution for 24 h before drying in the oven. The membrane porosity was reflected by weight difference per unit volume. At least three coupons of each membrane sheet were tested. The gel contents were measured by a solvent extraction method. The dry membrane was weighted and immersed in DMF for two weeks. After immersion, its dry weigh was measured again, and the gel content was calculated by the following Eq. (3):

Gel Content (%) = 
$$\frac{100 \times W_c}{W_a}$$
 (3)

where  $W_a$  and  $W_c$  were the dry weight of the crosslinked membrane before and after solvent extraction, respectively.

# 2.4. Solubility parameter calculations

Solubility parameters of the crosslinked polymer in this study were calculated to investigate the effect of Tris modification on mutual affinity between membranes and permeant solvent. The corresponding equation for the solubility parameter is

$$\delta^2 = \sqrt{\delta_d^2 + \delta_p^2 + \delta_h^2} \tag{4}$$

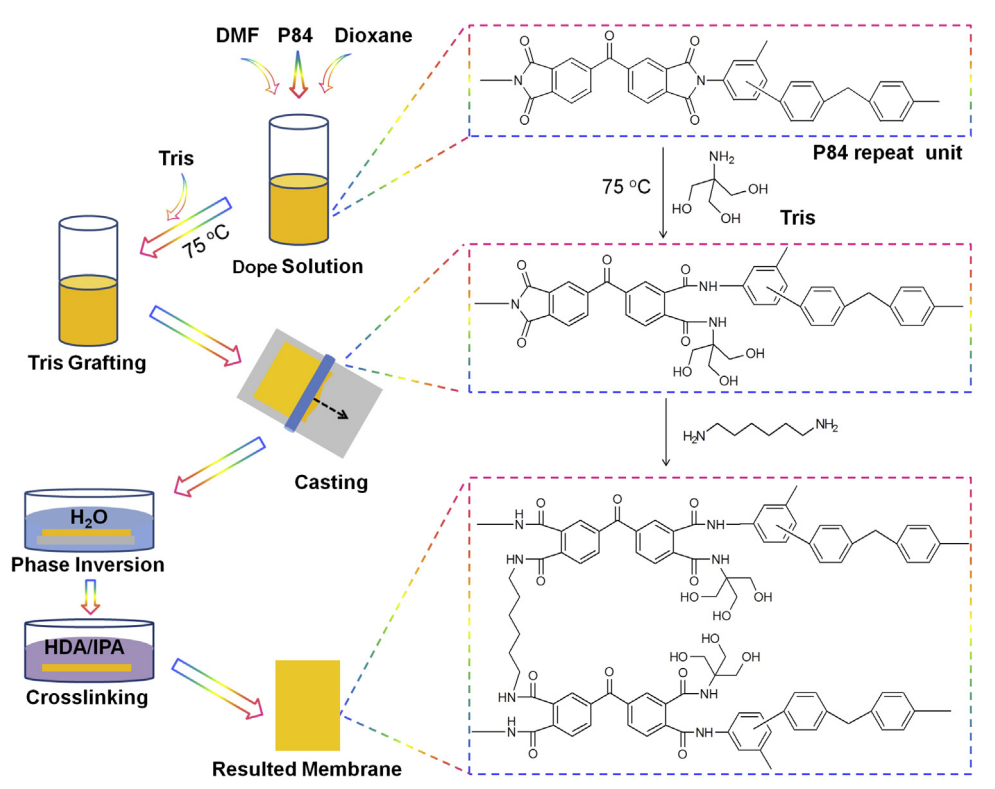


Fig. 1. Membrane fabrication protocol and the possible reaction mechanisms.

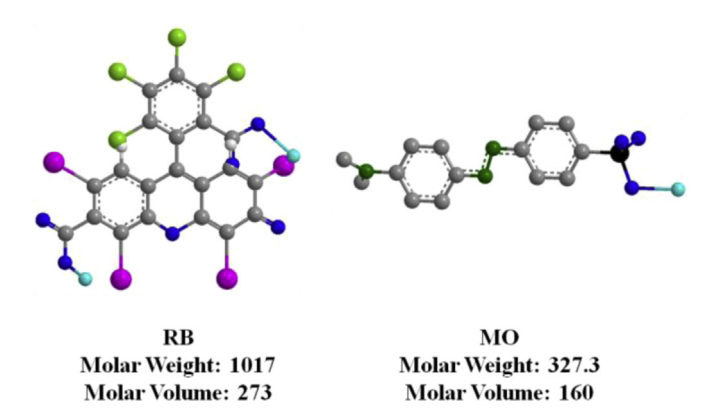


Fig. 2. Chemical structure, molar weight and molar volume of RB and MO.

where  $\delta_d$ ,  $\delta_p$  and  $\delta_h$  are the dispersion force, dipole and hydrogen bonding component of the solubility parameter, respectively. Furthermore,  $\delta_d$ ,  $\delta_p$  and  $\delta_h$  can be calculated by a group contribution method [32].

The solubility parameter distance Ra between membranes and solvent can be calculated as the following Eq. (5) [33]:

$$Ra = \sqrt{4(\delta_{d,M} - \delta_{d,S})^2 + (\delta_{p,M} - \delta_{p,S})^2 + (\delta_{h,M} - \delta_{h,S})^2}$$
(5)

Typically, a lower value of this parameter corresponds to a higher mutual affinity between membrane and permeant solvent.

#### 2.5. Nanofiltration experiments

The permeance and flux of NF membranes were measured with a self-made filtration apparatus (Fig. S1). Filtrations were performed in a stainless steel dead-end pressure cell with a 21.1 cm² active surface area. The operating pressure and temperature were kept at 5 bar and 25 °C with condensing apparatus. The feed solution was poured into the cell and stirred at 11.66 Hz (700 rpm) to minimize the possible concentration polarization. The feed solutions consisted of 35  $\mu$ M RB or MO (Fig. 2) in IPA or DMF. Solvent flux and permeance were obtained using Eqs. (6) and (7), respectively [34]:

$$F = \frac{V}{A \times t} \tag{6}$$

$$P = \frac{F_{\rm w}}{\Delta P} \tag{7}$$

where F is the solvent flux (L m<sup>-2</sup> h<sup>-1</sup>), V (L) is the volume of the solution penetrating through the membrane, A is the effective membrane area (m<sup>2</sup>), t is the operation time (h), P is permeance (L m<sup>-2</sup> h<sup>-1</sup> bar<sup>-1</sup>) and  $\Delta P$  is trans-membrane pressure (bar).

The solute rejections of the NF membranes were calculated by Eq. (8):

$$R = \left(1 - \frac{C_{\rm p}}{C_{\rm f}}\right) \times 100\% \tag{8}$$

where  $C_{\rm p}$  and  $C_{\rm f}$  are the solute concentrations in the permeate and the feed solution, respectively. The concentrations of RB in IPA were measured by a UV–vis Cintra20-GBC apparatus at a wavelength of 558 nm for RB and 422 nm for MO. At least three tests of each membrane sheet were performed.

#### 3. Results and discussion

#### 3.1. Basic characterizations

Based on the chemical mechanism of diamino crosslinking reaction [35], it is expected that the amine group in Tris can react with imide groups in polyimide to form amide group, while the hydroxyl groups should be kept and can tailor the physicochemical properties of resultant membranes. To prove our concept, the chemical characterizations have been carried out. Fig. 3 shows FT-IR spectra of pristine and Tris modified P84 membranes before and after diamino cross-linking. For membranes before/without crosslinking, the Tris modified P84 membrane (M4') exhibits an additional peak at 3400 cm<sup>-1</sup> comparing to pristine P84 membrane (M1'). It can be a merged peak from -OH of Tris and -NH- of the newly formed amide groups [36]. Appearance of stronger peak at 2925 cm $^{-1}$  is related to  $-CH_2$ - stretch [37] originating from Tris. After diamino crosslinking, the peak at 3400 cm<sup>-1</sup> shifts to 3260 cm<sup>-1</sup> and its intensity dramatically increases. This can be due to the increased proportion of -NH- band in the merged peak [35]. The peak at 2925 cm<sup>-1</sup> also becomes stronger in intensity after crosslinking, because of the introduction of -CH<sub>2</sub>- from HDA.

In addition, the spectra of the same membranes over the lower frequency range between  $1900~\rm cm^{-1}$  and  $1000~\rm cm^{-1}$  was magnified for analyzing the more detailed information. For membranes before crosslinking, the characteristic imide peaks of P84 membrane at  $1780~\rm cm^{-1}$ ,  $1718~\rm cm^{-1}$  and  $1352~\rm cm^{-1}$  [38–40] have gradually attenuated after Tris modification. Meanwhile, the typical amide peaks at  $1648~\rm cm^{-1}$  and  $1534~\rm cm^{-1}$  emerges.

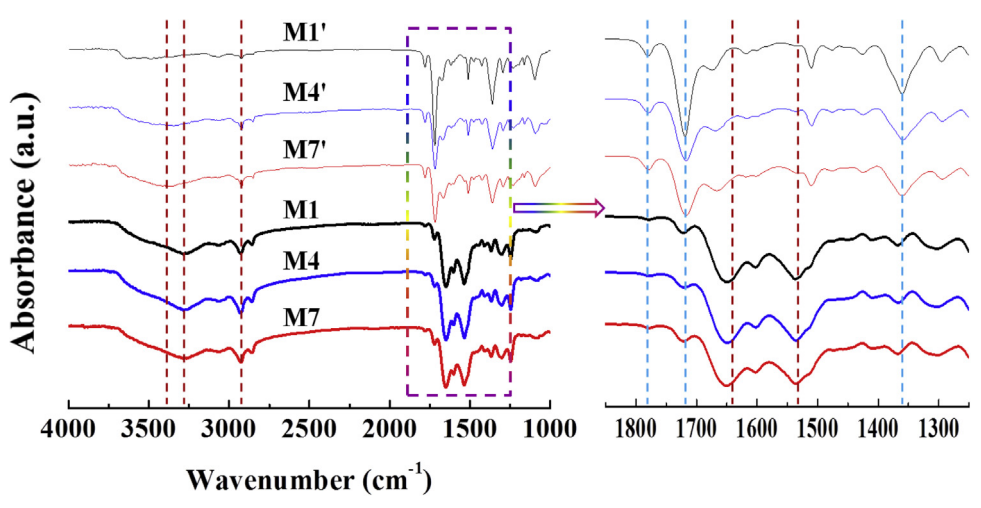


Fig. 3. FT-IR spectra of typical membranes. M1', M4' and M7' refer to corresponding membranes before crosslinking.

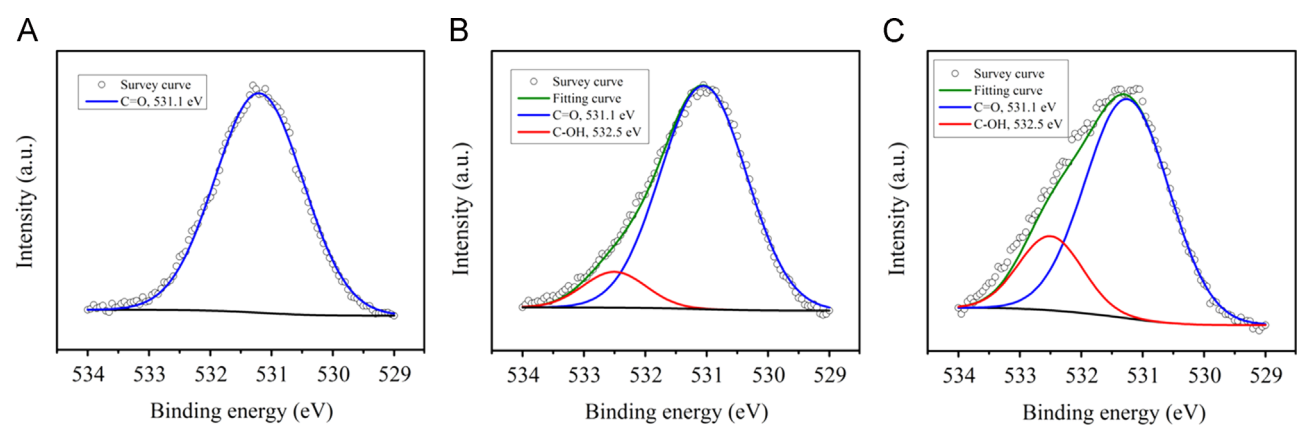


Fig. 4. The O1s spectra of the typical crosslinked membranes (A) M1, 0% Tris; (B) M4, 10% Tris; (C) M7, 20% Tris.

Increasing spectra intensity of the amide bands corresponds to the higher Tris loading. After cross-linking with HDA, all the membranes show a significantly stronger intensity of the amide characteristic peaks at 1648 cm<sup>-1</sup> and 1534 cm<sup>-1</sup>, and a weaker intensity of the imide (ring) characteristic peaks at 1780 cm<sup>-1</sup>, 1718 cm<sup>-1</sup> and 1352 cm<sup>-1</sup>. These results indicate that the cross-linking reaction has readily happened, and the Tris modification on the polymer chains does not interfere with the occurance of the crosslinking reaction.

Furthermore, a much detailed study on the membrane chemistry is investigated by employing XPS high-resolution scan of O1s spectra. The spectra of typical crosslinked membranes are scanned and deconvoluted as shown in Fig. 4. The peak at 531.1 eV is assigned to C=O in the crosslinked polyimide [41]. The newly emerged peak at 532.5 eV is associated to C-OH [42], and it increases with the Tris loading, proving the readily incorporation of Tris in membranes. Fig. 5 shows the schematic of the theoretical value calculation of the C-OH/C=O ratio  $(O_{II}/O_I)$ . In one Tris modified crosslinked P84 repeat unit, the number of O atom from carbonyl groups (marked in red circle) is 5, and the number of O atom form hydroxyl groups (marked in blue circle) is 6x (x is the molar ratio of Tris to imide). So the theoretical value of  $O_{II}/O_I$  can be calculated using Eq. (9):

$$O_{II}/O_{I} = 6x/5 \tag{9}$$

According to quantified XPS results shown in Table 2, the C-OH/C=O ratios of M4 (10% Tris) and M7 (20% Tris) membranes with fixed DMF:dioxane of 2:1 and varying Tris loading are 0.12 and 0.24, respectively. These results are well corresponding to the calculated theoretical values. Clearly, all the loaded Tris in the dope solution have taken part in chemical reaction completely.

Based on the analysis of FT-IR and XPS results, the possible reaction mechanisms of Tris modification and HDA crosslinking process have been proposed and shown in Fig. 1. It is worth pointing out that an elevated temperature (75 °C) of dope solution is crucial for the Tris modification reaction. A lower temperature leads to insufficient reaction. This can be explained by the following reasons: (1) the steric effect around amine group in Tris, originating from the –CH<sub>2</sub>OH structure, can hinder the reaction

**Table 2**The quantified analysis of O-containing groups.

Membrane	$O_I C=0$	O <sub>II</sub> C-OH	O <sub>II</sub> /O <sub>I</sub>		
	Composition (%)		Measured value	Theoretical value	
M1	100	0	0	0	
M4	89.53	10.47	0.12	0.12	
M7	80.65	19.35	0.24	0.24	

between amine and carbonyl groups of imide rings in P84; (2) the high viscosity (as discussed later) of dope solution can decrease the intermolecular collisions, inhibiting the reaction. With the increase of dope temperature, the steric effect around amine groups is weakened. In addition, the viscosity of dope solution will also decrease and the intermolecular collisions between Tris and P84 chains can be more intense, hence facilitating the reaction process. When the reaction temperature is too high, the possible side reaction may happen which deteriorates the modification efficiency [43,44].

The surface hydrophilicity of membrane can greatly affect the membrane performance in different solvents, especially for polar solvents such as IPA. In general, the smaller water contact angle indicates the better hydrophilicity of membranes. Table 3 illustrates the contact angles and surface energy results of various membranes. The pristine membrane (M1) has the water contact angle of 57°, which is similar to the value reported in the other literature [25]. The contact angle of membranes gradually decreases from 57° to 46° with the Tris loading (up to 20%). This phenomenon can be explained by the fact that the hydroxyl groups in Tris have been introduced onto the surface of polyimide membrane, which is validated by previous discussed FT-IR and XPS results. The influence of Tris modification on the membrane hydrophilicity is further elucidated by surface energy characterizations. Compared with pristine membrane, the Tris modified membranes show the higher total surface energies which gradually increase with the Tris loading. The main increment lies in the polar component of the total surface energies, emphasizing the key role of Tris modification on tailoring membrane hydrophilicity.

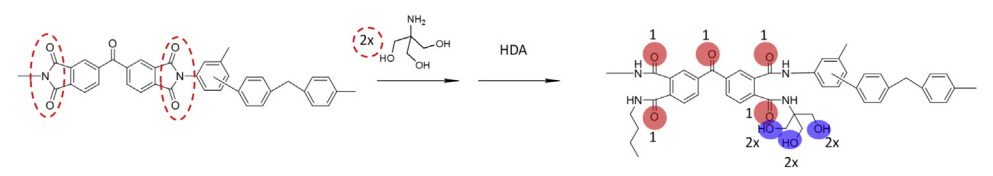


Fig. 5. The schematic of the theoretical value calculation of the C-OH/C=O ratio. (For interpretation of the references to color in this figure legend, the reader is referred to the web version of this article.)

**Table 3**Contact angles and surface energy of P84 OSN membranes modified with different Tris loading.

Membrane	Contact Angle (°)ª		Surface-ener	gy component	s (mJ m <sup>-2</sup> )
	Water	Diiodomethane	γL	$\gamma_L^d$	$\gamma_{\rm L}^{\rm p}$
M1	57	44	47.6	28.2	19.4
M2	54	43	49.6	28.2	21.4
M4	52	42	50.9	28.3	22.6
M6	48	40	53.7	28.6	25.1
M7	46	39	55.1	28.8	26.3

<sup>&</sup>lt;sup>a</sup> The error in contact angle measurement is no more than 1.5°.

Such improved hydrophilicity might be important for enhancing the solvent transport such as IPA.

The morphology of membrane is greatly influenced by the kinetic aspects of the phase inversion process (particularly the non-solvent/solvent diffusion rates). During phase inversion process, macrovoids are initiated by the nucleation of the polymer-lean

phase just below the skin layer of membrane [7]. In the instantaneous liquid–liquid demixing process, the diffusion rate of non-solvent into polymer phase greatly exceeds that of solvent into coagulation bath. Consequently, the large polymer concentration gradients occurs between the polymer solution and precipitated polymer solids, which generates the osmotic pressure in the nuclei as the driving force for the growth of macrovoids [33,45–47]. Therefore, the pristine membrane without Tris modification (M1) demonstrates a typical cross-sectional morphology of membrane prepared under instantaneous liquid–liquid demixing process, as shown in Fig. 6(A). It manifests a thin skin layer and a porous substructure with macrovoids.

On the other hand, in the delayed liquid–liquid demixing process, the diffusion rate of non-solvent into polymer phase is low, and the polymer concentration gradients are unable to generate sufficient osmotic pressure for the growth of macrovoids. In other words, the prior formed nuclei experience the same environment and more additional nuclei are newly formed, which limit the macrovoids growth and result in sponge-like pores [33,45–47]. Besides, it is well established that the viscosity of casting solution

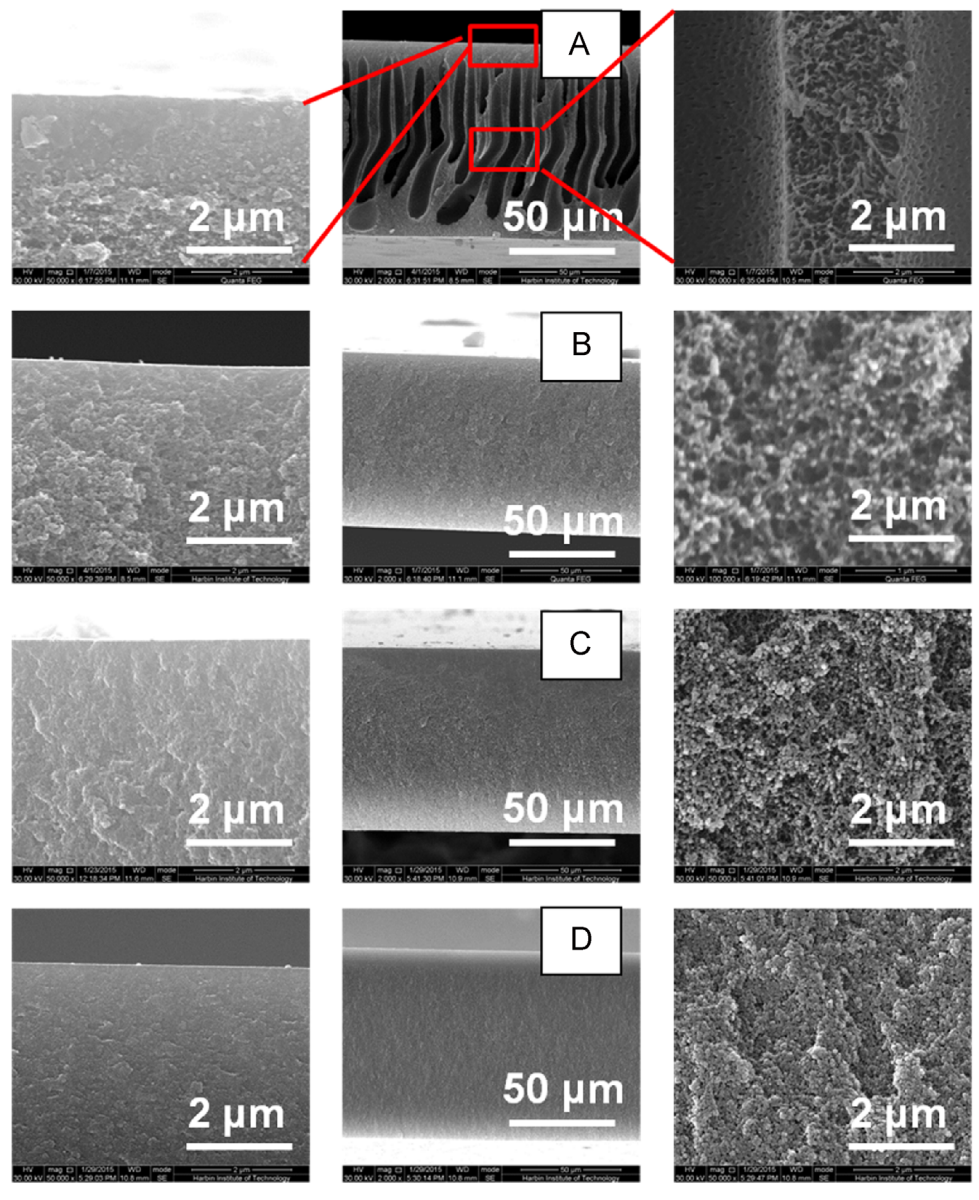


Fig. 6. SEM images of cross-sectional area of various Tris modified membranes fabricated with fixed DMF:dioxane ratio (2:1) and P84 concentration (22 wt%) (A) M1: 0% Tris; (B) M2: 5% Tris; (C) M4: 10% Tris; (D) M7: 20% Tris.

**Table 4** Viscosity of dope solutions at 20 °C.

P84 wt%	DMF:dioxane	Tris:Imide (%)				
		0	5	10	15	20
		Viscosity (mPa s)				
22	2:1	4030	4620	7680	12,500	15,600
	1:1	5040		10,100		
	3:1	3730		6720		
20	2:1	2050		3560		
24	2:1	8010		17,800		

tends to form a barrier for the diffusion of water into polymer solution during phase inversion, thus slowing down the non-solvent/solvent diffusion rate and turning the instantaneous liquid-liquid demixing process into a delayed one [48,49]. As shown in Fig. 6(B), the membrane with 5% Tris modification (M2) shows a dramatically morphological evolution compared to M1. The thicker top-layer and inter-connected sponge-like pores in M2 have

readily formed compared to the thin top-layer and macrovoids in M1, which can be ascribed to the higher dope solution viscosity, as shown in Table 4. The dope solution viscosity increases with the Tris loading. This can be attributed to the intramolecular and intermolecular hydrogen bonding among the hydroxyl groups introduced to the polymer chains and the enhanced polymer chain entanglement [50–52]. Increasing the dope solution viscosity leads to a more pronounced barrier effect during phase inversion, and the magnified top and middle section morphologies of membranes imply that the top-layer becomes thicker. Meanwhile, the size of sponge-like pores gradually shrinks and the sub-layer becomes denser with the Tris loading. Further increasing the Tris loading more than 20% is not practical as the dope solution is too viscous, resulting in the casting problems.

Fig. 7 shows the cross-sectional morphology of M10, M11, M14 and M15. Comparing M10 (Fig. 7(A), DMF:dioxane of 1:1, 0% Tris) with M1 (Fig. 6(A), DMF:dioxane of 2:1, 0% Tris), it is obvious to notice an decrease in macrovoids structure with decreasing DMF: dioxane ratio. This result is consistent with the literature reported by See-Toh et al. [53]. When decreasing DMF:dioxane ratio for

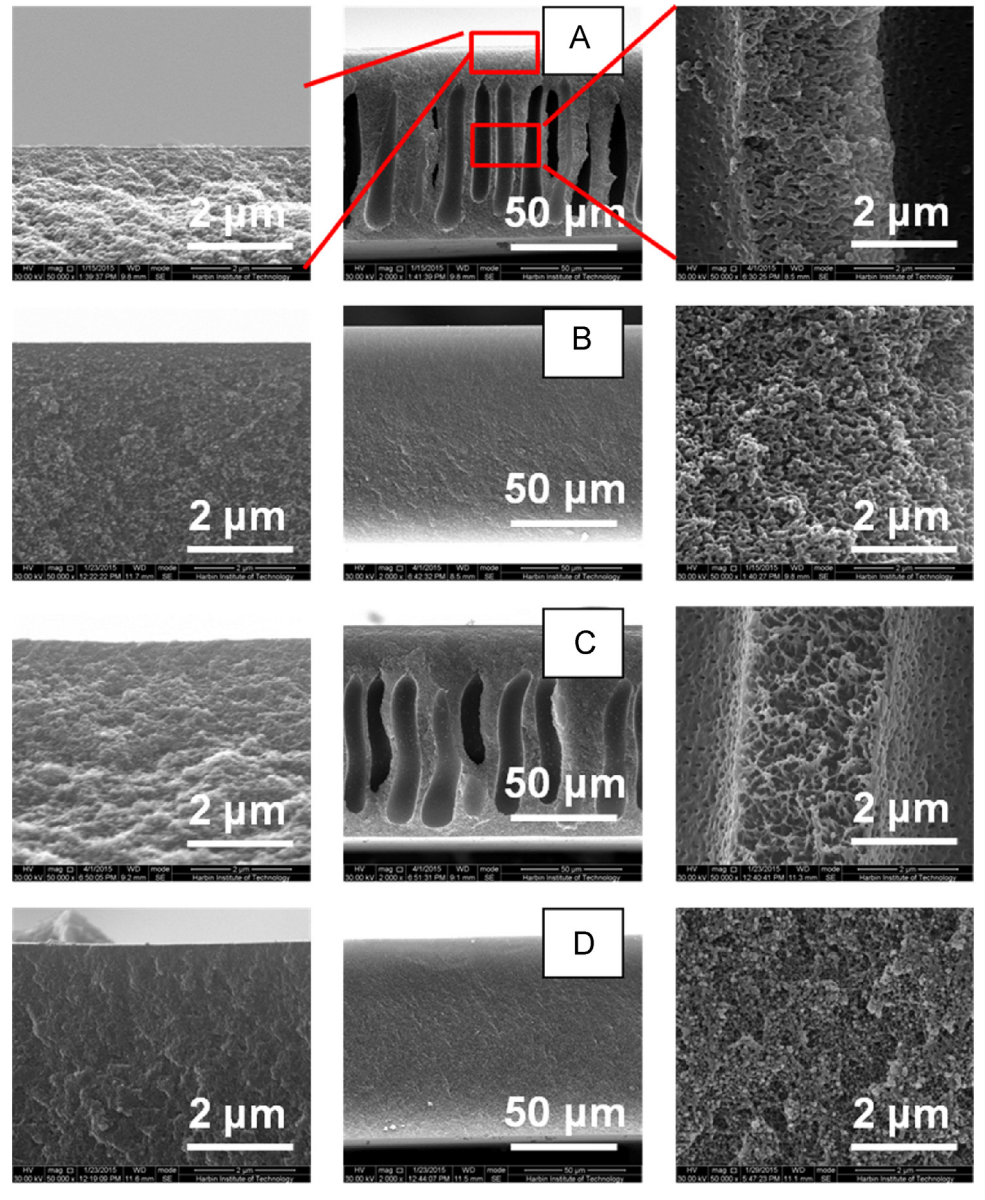
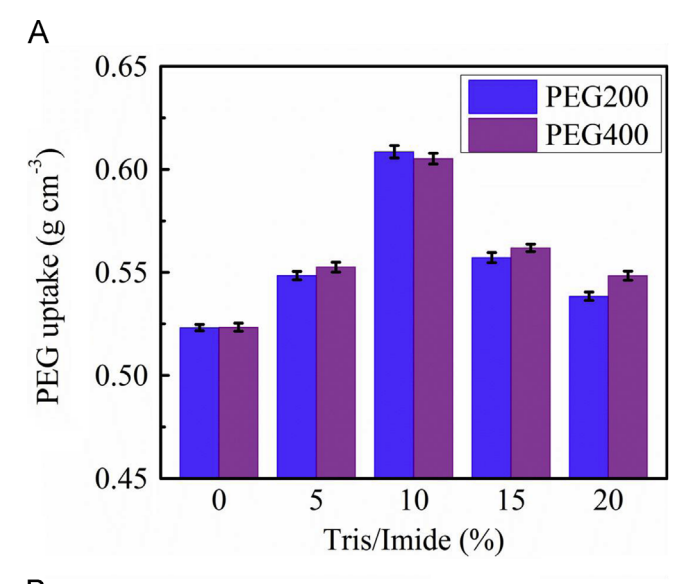


Fig. 7. SEM images of cross-sectional area of membranes (A) M10: 22 wt% P84, 1:1 DMF:dioxane, 0% Tris; (B) M11: 22 wt% P84, 1:1 DMF:dioxane, 10% Tris; (C) M14: 24 wt% P84, 2:1 DMF:dioxane, 0% Tris; (D) M15: 24 wt% P84, 2:1 DMF:dioxane, 10% Tris.



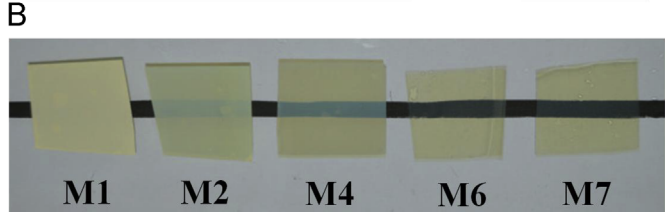


Fig. 8. (A) PEG uptake, and (B) transparency observation of typical membranes.

preparing Tris modified membranes of M4 (Fig. 6(C), DMF:dioxane of 2:1, 10% Tris) and M11 ((Fig. 7(B), DMF:dioxane of 1:1, 10%Tris), the sub-layer become more dense. These are possibly due to (1) dioxane has a lower affinity towards water than DMF, and the presence of dioxane as co-solvent decreases the diffusional driving force of non-solvent/solvent diffusion [53]; (2) the increased viscosity of casting solution, especially for the Tris modified casting solutions (Table 4), further slows down the non-solvent/solvent diffusion rate during the phase inversion process. Both the two factors attribute to the shift of phase inversion process from the instantaneous phase inversion to the delayed phase inversion. In addition, the higher polymer concentration contributes to the suppressed macrovoids (M1 and M14) or denser sub-layer (M4 and M15).

Fig. 8(A) shows the PEG uptake of membranes with various Tris loadings. The PEG200 uptake increases with Tris loading from 0% to 10%, indicating a higher porosity of M4. Jimenez-Solomon et al. have also reported that a P84 membrane with sponge-like pores has the higher porosity than that with macrovoids [31]. Further increasing the Tris loading above 10% results in a declined PEG200 uptake, which could be due to the gradually denser sub-layers. In addition, the PEG400 uptake has no significant difference with PEG200 uptake, suggesting the porosity obtained by this method is not obviously affected by the molecular size of used PEG.

Interestingly, we find that the Tris modified membranes are transparent, and the transparency can be improved by increasing the Tris loading, as shown in Fig. 8(B). Transparent polyimide membranes have been reported previously [54–56], which suggest the viscosity of dope solution is responsible for the transparency. Basically, a viscous dope solution leads to the smaller sponge-like pores and the small size of these pores probably below the wavelength of light would endorse the membrane with the better transparency.

**Table 5**Solubility parameters of typical membranes, IPA and DMF.

Entry	Tris/Imide	Solubility	Solubility parameter (MPa <sup>1/2</sup> )			
		$\delta_{ m d}$	$\delta_{ m p}$	$\delta_{ m h}$	δ	
M1	0	17.42	6.19	7.58	19.98	
M2	5%	17.40	6.18	8.05	20.14	
M4	10%	17.38	6.16	8.49	20.30	
M6	15%	17.36	6.15	8.90	20.45	
M7	20%	17.34	6.14	9.29	20.61	
IPA		15.8	6.1	16.4	23.5	
DMF		17.4	13.7	11.3	24.8	

# 3.2. Membrane-solvent mutual affinity

The membrane-solvent mutual affinity can be reflected by the solubility parameter. In this study, we tend to investigate the relationship between membrane-solvent mutual affinity and membrane performance. Table 5 lists the solubility parameter of typical crosslinked P84, IPA [57] and DMF [57]. When increasing Tris loading, the dispersion force component and dipole component decrease slightly, while the hydrogen bonding component increases significantly, contributing to an increased total solubility parameter. The solubility parameter distance between membrane and solvent, Ra<sub>M-S</sub>, is calculated and demonstrated in Fig. 9. It exhibits that although both Ra<sub>M-IPA</sub> and Ra<sub>M-DMF</sub> decrease with the Tris loading, the decrement of Ra<sub>M-IPA</sub> is much larger than that of Ra<sub>M-DMF</sub>, indicating the membrane-IPA mutual affinity may be more responsive to Tris modification than that of membrane-DMF.

# 3.3. Nanofiltration experiments

In fact, we have screened out some common monoamines based on the nanofiltration performance firstly, and find Tris can give the best membrane performance after modification (Figs. S3–S5). Therefore, Tris is specially chosen for this study.

# 3.3.1. Effects of Tris loading on the membrane performance

Fig. 10(A) shows the membrane performance for the RB removal from IPA solution with aspect to different Tris loadings. P84 concentration and DMF:dioxane ratio are fixed at 22% and 2:1, respectively. When initially increasing Tris loading from 0% to 10%, IPA permeance significantly increases to 270% of the original value from  $1.00 \, \text{L m}^{-2} \, \text{h}^{-1} \, \text{bar}^{-1}$  (at 0%) to  $2.70 \, \text{L m}^{-2} \, \text{h}^{-1} \, \text{bar}^{-1}$  (at 10%). However, further increasing Tris loading results in the decline of IPA permeance. In fact, there are two main reasons for the significantly enhanced IPA permeance at the initiate stage: (1) the membrane-IPA mutual affinity is improved with the Tris loading,

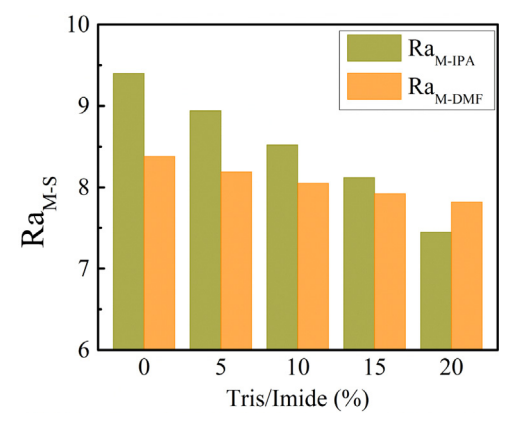


Fig. 9. Solubility parameter distance between membranes and IPA or DMF.

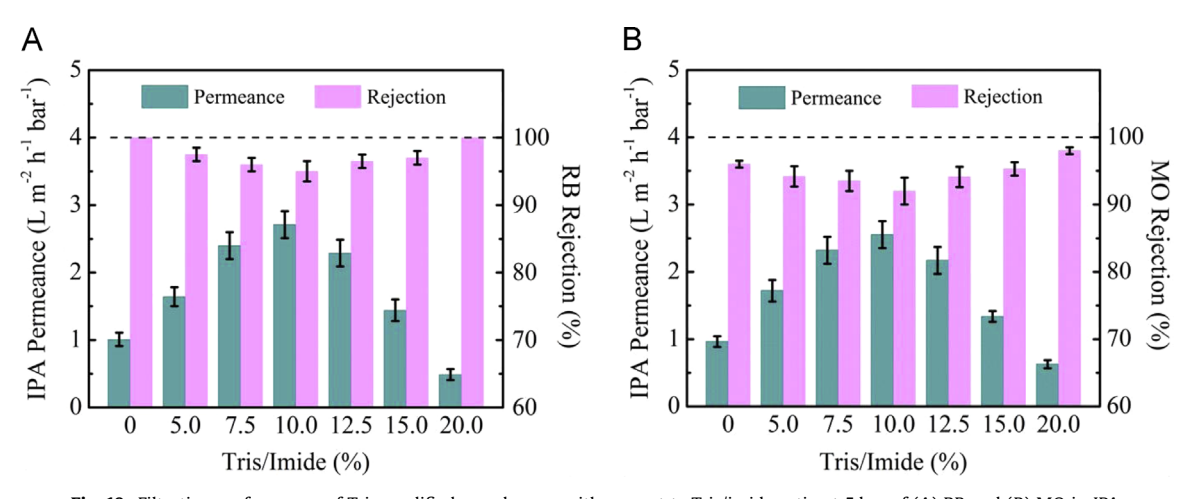


Fig. 10. Filtration performance of Tris modified membranes with respect to Tris/imide ratio at 5 bar of (A) RB and (B) MO in IPA.

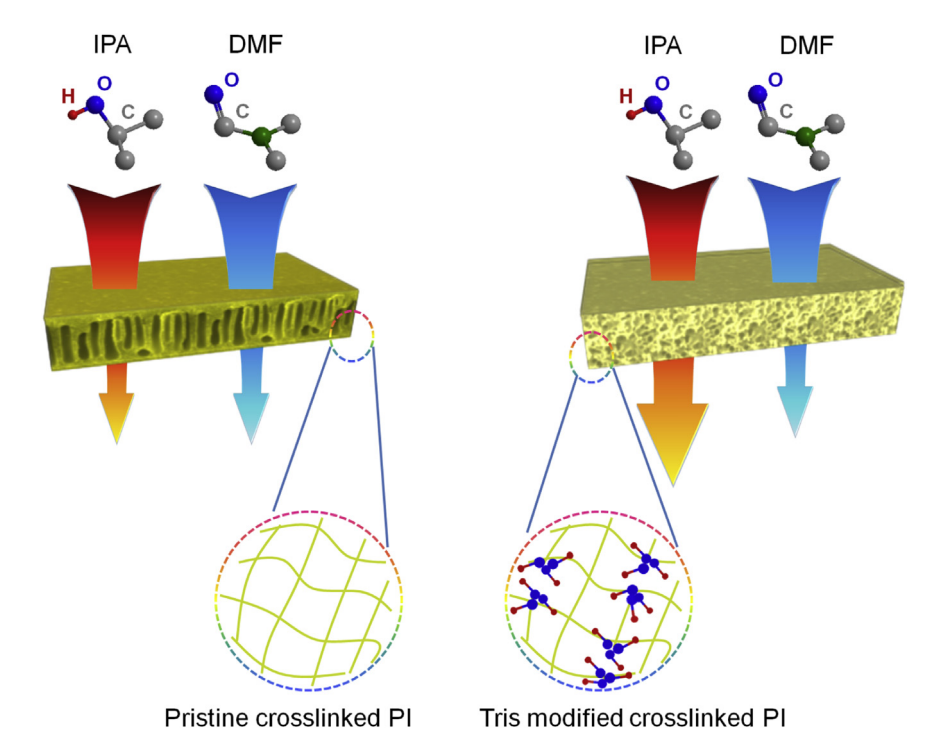


Fig. 11. Schematic of the membrane morphologies and solvent permeation performance of pristine and Tris modified PI OSN membranes.

as reflected by the decreased Ra<sub>M-IPA</sub>. This can help reduce the permeation resistance and facilitate IPA transport; (2) the high porosity of the sponge-like structure in Tris modified membranes may also lead to IPA permeance increase because PI membrane with the higher porosity gives a less tortuous path for a given solvent to permeate through [31,58,59]. The schematic of the IPA permeance performance and the membrane morphologies of pristine and Tris modified membranes are shown in Fig. 11. Gao et al. reported an analogous water flux increase of poly (L-lactic acid) UF membrane with sponge-like pores compared with figurelike pores, and they explain that the better connectivity between sponge-like pore walls is beneficial to the water transmittance [49]. However, when further increasing the Tris loading (  $\geq$  12.5%), the skin layer will become thicker, which can increase the IPA permeation resistance. Besides, the excessive hydrogen bond can reduce polymer chain flexibility and limit the swelling degrees of the polymer in solvent. Thus, the IPA permeance decreases at the much higher Tris loading. The rejection of RB slightly decreases from 99.5% to 95% when initially increasing Tris loading from 0% to

10%. Then, the RB rejection increases up to 100% when further increasing Tris loading to 20%. These may be due to the dragging of solvent at the high solvent permeance [60].

Further study illustrates there is no obvious difference in IPA permeance between the separation of RB and MO from IPA solutions. The MO rejection trend varying with the Tris loading is similar to that of RB. But the MO rejection is lower than RB rejection under the same conditions, which is due to the relatively smaller molecular size of MO (160 cm<sup>3</sup> mol<sup>-1</sup>) than that of RB (273 cm<sup>3</sup> mol<sup>-1</sup>) [60].

Fig. 12 shows the effect of different Tris loadings on the membrane performance for the RB removal from DMF solution. According to Fig. 12, the DMF permeance continuously decreases and the dye rejection (RB or MO) continuously increases with the Tris loading. For example, the DMF permeance decreases from  $6.07 \, \text{L m}^{-2} \, \text{h}^{-1} \, \text{bar}^{-1}$  to  $1.44 \, \text{L m}^{-2} \, \text{h}^{-1} \, \text{bar}^{-1}$ , and the RB rejection increases from 95.3% to 100% when increasing Tris loading from 0% to 20%. Further analysis illustrates that the DMF permeance decline happens mainly at the higher Tris loading ranging

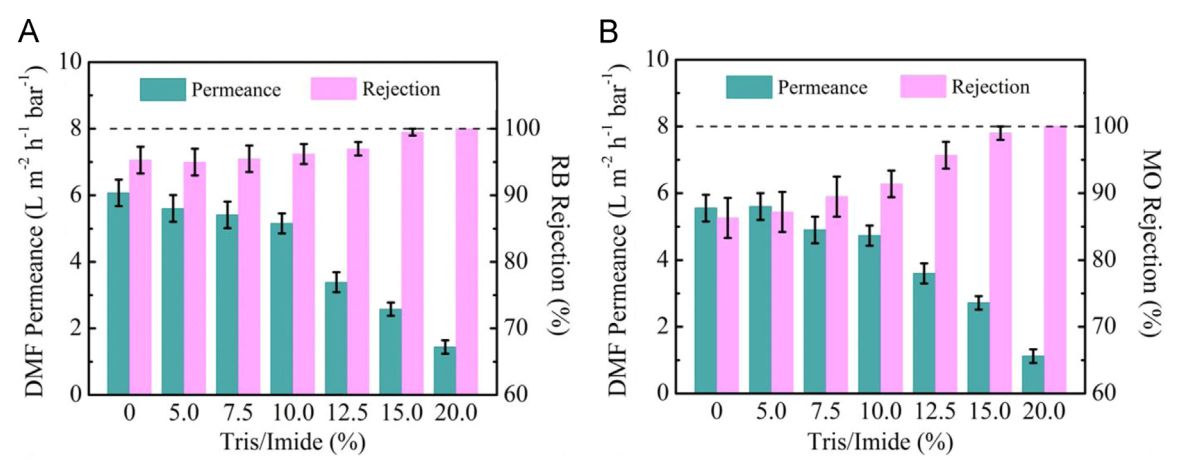


Fig. 12. Filtration performance of Tris modified membranes with respect to Tris/imide ratio at 5 bar of (A) RB and (B) MO in DMF.

from 10% to 20%. Due to the limited enhancement on membrane-DMF mutual affinity (Fig. 9), the Tris modification has no significant promoting effect on DMF transport. As the skin layer is becoming thicker, the permeate resistance tends to increase. Therefore, the DMF permeance continuously decreases.

Typically, the IPA permeance is lower than DMF permeance for the same membrane. For instance, the IPA permeance of M1 in the separation of RB from IPA ( $1.00 \, \text{L m}^{-2} \, \text{h}^{-1} \, \text{bar}^{-1}$ ) is much lower than the corresponding DMF permeance ( $6.08 \, \text{L m}^{-2} \, \text{h}^{-1} \, \text{bar}^{-1}$ ). Several factors can be related to the difference permeance, including membrane-solvent interactions and physical properties of solvent (molar volume and viscosity, *etc.*) [15, 61]. Since IPA has a similar molar volume ( $76.9 \, \text{cm}^3 \, \text{mol}^{-1}$ ) to that of DMF

(77.43 cm³ mol<sup>-1</sup>), the higher viscosity of IPA (2.044 mpa s) than DMF viscosity (0.802 mpa s) may attribute to the lower IPA permeance [8]. The rejection of dyes in IPA is higher than that in DMF at any Tris loading, and this may be due to the different size and shape (hydrodynamic radius) of dyes in various solvents. However, a further research on this behavior is beyond the scope of this work.

3.3.2. Effects of DMF:dioxane ratios on the membrane performance
The variation of the solvent:co-solvent ratio in dope solution
may control the performance of the resultant membranes
[53,62,63]. We are intrigued whether this principle is generally
applied to the Tris modified membranes. For comparison, the

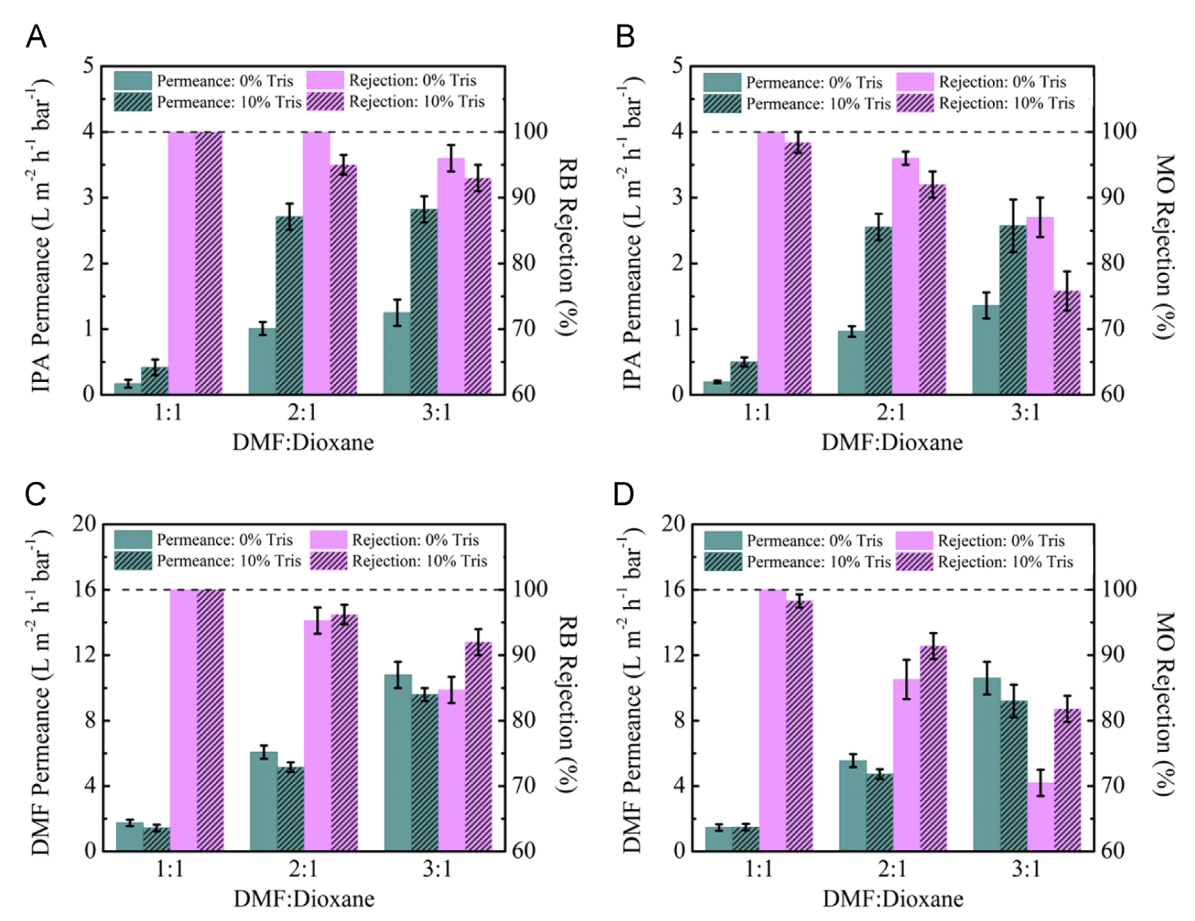


Fig. 13. Filtration performance of Tris modified membranes with respect to DMF:dioxane ratio at 5 bar of RB and MO in IPA ((A) and (B)) or DMF ((C) and (D)).

pristine membranes are also investigated in this section. The results of the dye removal from IPA solution with the membranes fabricated by varying DMF:dioxane ratios are shown in Fig. 13 (A) and (B). Both the pristine and modified membranes show the higher IPA permeance and lower dye rejections with increasing DMF:dioxane ratio. It is worth noting that the permeance of modified membranes have increased to 385%, 270% and 226% of the corresponding original values at DMF:dioxane ratio of 1:1, 2:1 and 3:1, respectively. This phenomenon can be explained based on the pore size and solvent-membrane interactions differences. For membranes prepared at a DMF:dioxane ratio of 3:1 (M8 without Tris and M9 with 10% Tris loading), the top layers are relatively "looser" and the membrane structures are more "open". Therefore, the IPA permeate resistance becomes less and the enhancing effect of hydroxyl groups on IPA permeance is not so obvious. For membranes prepared at a DMF: dioxane ratio of 1:1, M10 and M11, the top layer are relatively "tighter" and the membranes structures are "close". Thus more IPA molecular can interact with the hydroxyl groups on the polymer chains for solvent permeation and the enhancing effect of hydroxyl groups on IPA permeance is more

Fig. 13(C) and (D) show the removal of dyes from DMF solution. The modified membranes show a slight decline in DMF permeance than the corresponding pristine membranes. The DMF permeance has decreased to 82%, 85% and 89% of the corresponding original values at the DMF/dioxane ratios of 1:1, 2:1 and 3:1, respectively, which might be attributed to the increasing tighter top-layers. Accordingly, the dyes rejections increase as the proportion of dioxane in the mixed solvent increases.

3.3.3. Effect of P84 concentrations on the membrane performance

The IPA fluxes and RB rejections of both pristine and Tris modified membranes prepared with various P84 concentrations are shown in Fig. 14(A). Unexpectedly, the Tris modified membrane shows a lower permeance than the pristine membrane at 20% P84 concentration, although both the Tris modified membranes and pristine membranes demonstrate the declined permeance and enhanced dye rejections when increasing P84 concentration. The IPA permeance of Tris modified membrane decreases to 88% of the original value at 20% P84 concentration. However, when further increasing P84 concentration to 22% and 24%, the IPA permeance of Tris modified membrane can increase to 270% and 330% of the corresponding original values, respectively. For the pristine membrane, the membrane structure formed at 20% P84 concentration is much open than that formed at the higher P84 concentrations, as reflected by the obviously higher IPA permeance. It is the pore size, rather than the membrane hydrophilicity, dominating the IPA permeance at lower P84 concentration. The Tris modification of membrane makes the pore size shrink, thus decreasing the IPA permeance at lower P84 concentration. When increasing P84 concentration, the membrane structures become close and the enhanced hydrophilicity can gradually improve solvent permeance.

Fig. 14(C) and (D) shows the dye removal from DMF solutions at different P84 concentrations. The modified membrane shows a slight lower DMF permeance than the corresponding pristine membrane at any P84 concentration. For example, the DMF permeance decreases to 72%, 85% and 92% of the corresponding original values after Tris modification at 20%, 22% and 24% P84 concentration, respectively. This could be due to DMF permeance is primarily dominated by the membrane pore size, and the

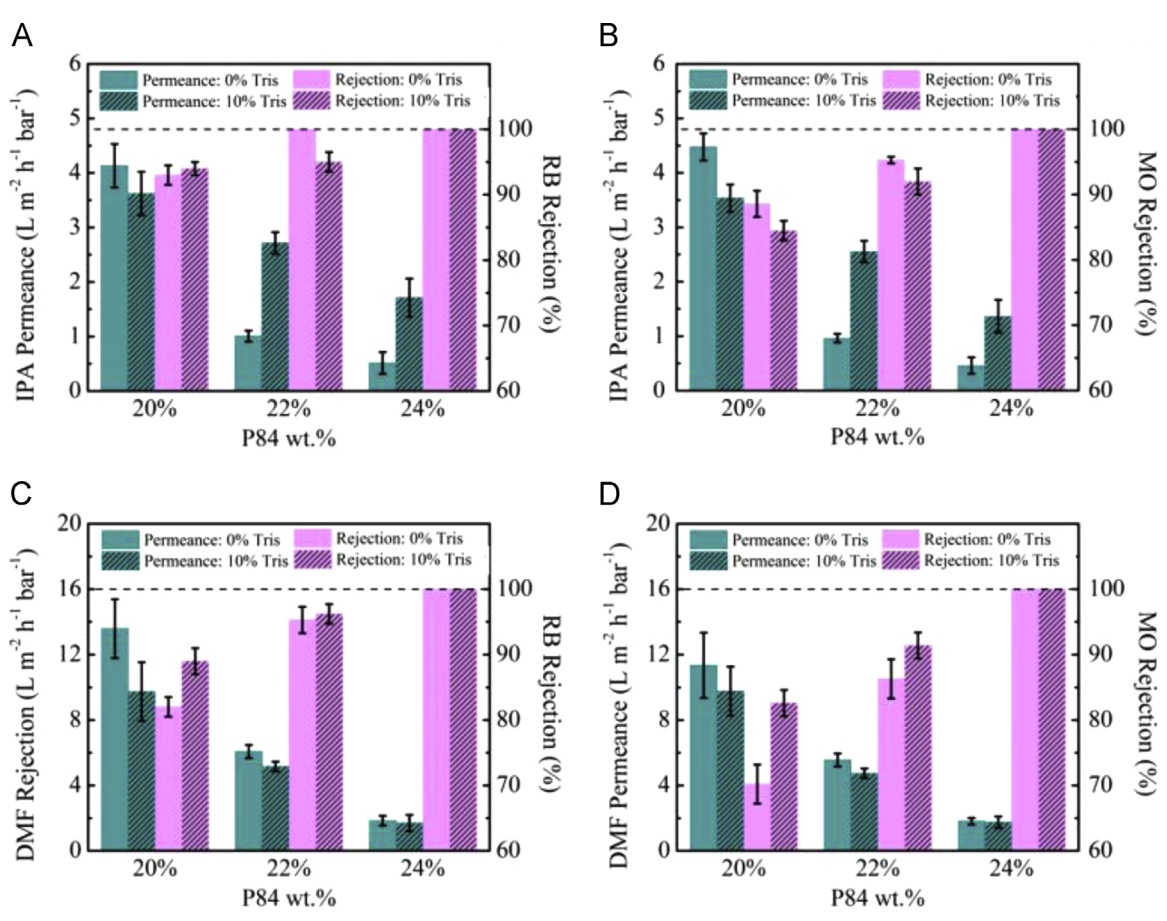


Fig. 14. Filtration performance of Tris modified membranes with respect to P84 concentrations at 5 bar of RB and MO in IPA ((A) and (B)) or DMF ((C) and (D)).

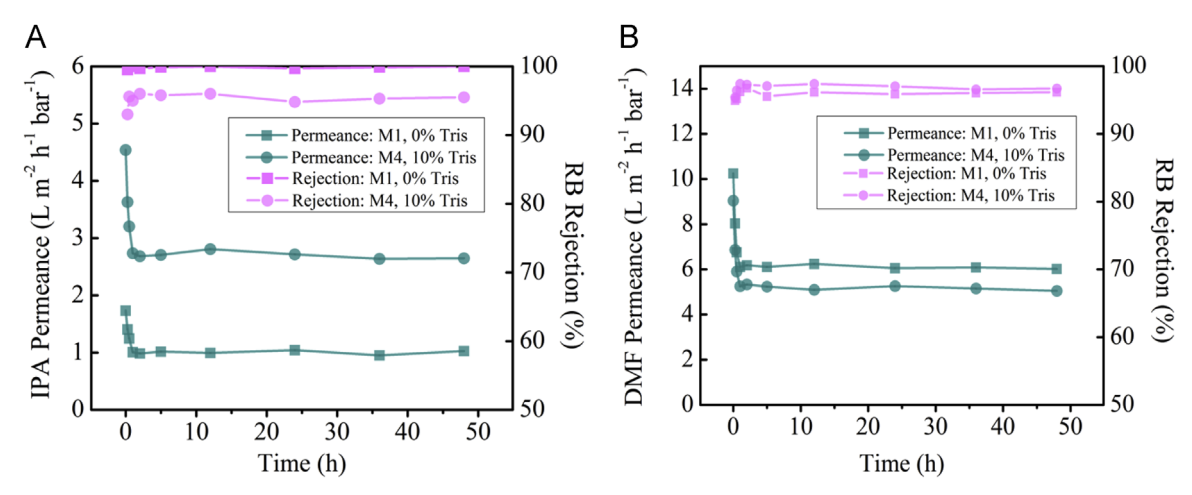


Fig. 15. Filtration performance of M1 and M4 in a 48 h long-term run for RB removal from (A) IPA and (B) DMF.

decreased pore size after Tris modification is more evident at lower P84 concentration.

# 3.3.4. Stability and long-term performance

Gel content was measured to assess the stability of crosslinked membranes. It is found that all the membranes (M1–M15) have the gel content higher than 98% after soaking in DMF for two weeks, indicating the good stabilities of these membranes. The long-term performance [64] of the Tris modified membrane M4 and the pristine membrane M1 were specially tested in around 48 h in a dead-end filtration using solutions of RB in IPA and DMF as feed. As shown in Fig. 15, both solvent permeance and RB rejection of M4 were stable after an initial period of membrane compaction [65,66]. These results indicate the membranes exhibit good stability over a long-term period whilst still maintaining the excellent separation performances.

# 4. Conclusions

In conclusion, we have designed a novel strategy to enhance the performance of polyimide OSN membrane for sustainable applications by monoamine (Tris) modification. Tris modified polyimide OSN membranes have been prepared by adding Tris to the dope solution before phase inversion and diamino crosslinking. The Tris modification has resulted in an increased hydrophilicity and a sponge-like membrane matrix. The IPA permeance has increased to 270% of the original value with a merely decline (less than 5%) in dyes rejection under optimized conditions. The solubility parameter distance has been calculated to explain the different trend of IPA and DMF permeance. The improvement of IPA permeance is more significant at the lower DMF: dioxane ratio and higher P84 concentration. Moreover, the Tris modified membrane showed good stability and excellent separation performances over a 48 h long-term run in harsh organic solvent. The monoamine modification presented in this study provides a novel strategy to manipulate membrane-solvent interactions and improve solvent permeance simply by choosing an appropriate monoamine for modification. We believe that the discovered versatile approach have great potential for sustainable applications.

# Acknowledgments

This work was supported by National Natural Science Foundation of China (U1462103, 21177032), Program for New Century

Excellent Talents in University (NCET-11-0805), the Fundamental Research Funds for the Central Universities (Grant no. HIT.BRE-TIV.201307), Harbin Science and Technology Innovation Talent Funds (2014RFXXJ028) and State Key Laboratory of Urban Water Resource and Environment (Harbin Institute Technology) (No. 2014DX05). Special thanks to Pro. Yuyan Liu from Harbin Institute of Technology for help on viscosity measurement.

# Appendix A. Supplementary material

Supplementary data associated with this article can be found in the online version at http://dx.doi.org/10.1016/j.memsci.2015.09. 029.

# References

- P. Marchetti, M.F.J. Solomon, G. Szekely, A.G. Livingston, Molecular separation with organic solvent nanofiltration: a critical review, Chem. Rev. 114 (2014) 10735–10806.
- [2] X.Q. Cheng, Y.L. Zhang, Z.X. Wang, Z.H. Guo, Y.P. Bai, L. Shao, Recent advances in polymeric solvent-resistant nanofiltration membranes, Adv. Polym. Sci. 33 (21455) (2014) E1–E24.
- [3] P. Vandezande, L.E.M. Gevers, I.F.J. Vankelecom, Solvent resistant nanofiltration: separating on a molecular level, Chem. Soc. Rev. 37 (2008) 365–405.
- [4] L. Shao, X.Q. Cheng, Z.X. Wang, J. Ma, Z.H. Guo, Tuning the performance of polypyrrole-based solvent-resistant composite nanofiltration membranes by optimizing polymerization conditions and incorporating graphene oxide, J. Membr. Sci. 452 (2014) 82–89.
- [5] J. Campbell, G. Székely, R.P. Davies, D.C. Braddock, A.G. Livingston, Fabrication of hybrid polymer/metal organic framework membranes: mixed matrix membranes versus in suit growth, J. Mater. Chem. A 2 (2014) 9260–9271.
- [6] S. Loeb, S. Sourirajan, Sea water demineralization by means of an osmotic membrane, Adv. Chem. Ser. 38 (1963) 117–132.
- [7] Y.H. See-Toh, F.W. Lim, A.G. Livingston, Polymeric membranes for nanofiltration in polar aprotic solvents, J. Membr. Sci. 301 (2007) 3–10.
- [8] K. Vanherck, P. Vandezande, S.O. Aldea, I.F.J. Vankelecom, Cross-linked polyimide membranes for solvent resistant nanofiltration in aprotic solvents, J. Membr. Sci. 320 (2008) 468–476.
- [9] K. Hendrix, K. Vanherck, I.F.J. Vankelecom, Optimization of solvent resistant nanofiltration membranes prepared by the in-situ diamine crosslinking method, J. Membr. Sci. 421–422 (2012) 15–24.
- [10] H. Siddique, E. Rundquist, Y. Bhole, L.G. Peeva, A.G. Livingston, Mixed matrix membranes for organic solvent nanofiltration, J. Membr. Sci. 452 (2014) 354–366.
- [11] K. Vanherck, G. Koeckelberghs, I.F.J. Vankelecom, Crosslinking polyimides for membrane applications: a review, Prog. Polym. Sci. 38 (2013) 874–896.
- [12] L. Shao, T.S. Chung, S.H. Goh, K.P. Paramoda, Polyimide modification by a linear aliphatic diamine to enhance transport performance and plasticization resistance, J. Membr. Sci. 256 (2005) 46–56.
- [13] L. Shao, T.S. Chung, S.H. Goh, K.P. Paramoda, The effects of 1,3-cyclohexanebis (methylamine) modification on gas transport and plasticization resistance of polyimide membranes, J. Membr. Sci. 267 (2005) 78–89.
- [14] L. Shao, L. Liu, S.X. Cheng, Y.D. Huang, J. Ma, Comparison of diamino cross-

- linking in different polyimide solutions and membranes by precipitation observation and gas transport, J. Membr. Sci. 312 (2008) 174–185.
- [15] D. Bhanushali, S. Kloos, C. Kurth, D. Bhattacharyya, Performance of solventresistant membranes for non-aqueous systems: solvent permeation results and modeling, J. Membr. Sci. 189 (2001) 1–21.
- [16] P. Silva, S. Han, A.G. Livingston, Solvent transport in organic solvent nanofil-tration membranes, J. Membr. Sci. 262 (2005) 49–59.
- [17] A.V. Volkov, V.V. Parashchuk, D.F. Stamatialis, V.S. Khotimsky, V.V. Volkov, M. Wessling, High permeable PTMSP/PAN composite membranes for solvent nanofiltration, J. Membr. Sci. 333 (2009) 88–93.
- [18] S. Tsarkov, V. Khotimskiy, P.M. Budd, V. Volkov, J. Kukushkina, A. Volkov, Solvent nanofiltration through high permeability glassy polymers: Effect of polymer and solute nature, J. Membr. Sci. 423–424 (2012) 65–72.
- [19] İ.F.J. Vankelecom, K.D. Smet, L.E.M. Gevers, A.G. Livingston, D. Nair, S. Aerts, S. Kuypers, P.A. Jacobs, Physico-chemical interpretation of the SRNF transport mechanism for solvents through dense silicone membranes, J. Membr. Sci. 231 (2004) 99–108.
- [20] J.A. Wesselingh, A.M. Bollen, Multicomponent diffusivities from the free volume theory, Trans. IChemE 75 (1997) 590–602.
- [21] R. Krishna, J.A. Wesselingh, The Maxwell–Stefan approach to mass transfer, Chem. Eng. Sci. 52 (1997) 861–911.
- [22] P. Schmidt, E.L. Bednarz, P. Lutze, A. Górak, Characterisation of organic solvent nanofiltration membranes in multi-component mixtures: process design workflow for utilising targeted solvent modifications, Chem. Eng. Sci. 115 (2014) 115–126.
- [23] S. Postel, G. Spalding, M. Chirnside, M. Wessling, On negative retentions in organic solvent nanofiltration, J. Membr. Sci. 447 (2013) 57–65.
- [24] H.J. Zwijnenberg, S.M. Dutczak, M.E. Boerrigter, M.A. Hempenius, M.W. J. Luiten-Olieman, N.E. Benes, M. Wessling, D. Stamatialis, Important factors influencing molecular weight cut-off determination of membranes in organic solvents, J. Membr. Sci. 390–391 (2012) 211–217.
- [25] H. Siddique, Y. Bhole, L.G. Peeva, A.G. Livingston, Pore preserving crosslinkers for polyimide OSN membranes, J. Membr. Sci. 465 (2014) 138–150.
- [26] I. Soroko, A.G. Livingston, Impact of TiO<sub>2</sub> nanoparticles on morphology and performance of crosslinked polyimide organic solvent nanofiltration (OSN) membranes, J. Membr. Sci. 343 (2009) 189–198.
- [27] D.W. Mangindaan, N.M. Woon, G.M. Shi, T.S. Chung, P84 polyimide membranes modified by a tripodal amine for enhanced pervaporation dehydration of acetone, Chem. Eng. Sci. 122 (2015) 14–23.
- [28] K. Vanherck, A. Cano-Odena, G. Koeckelberghs, T. Dedroog, I.F.J. Vankelecom, A simplified diamine crosslinking method for PI nanofiltration membranes, J. Membr. Sci. 353 (2010) 135–143.
- [29] L. Shao, T.S. Chung, S.H. Goh, K.P. Pramoda, Transport properties of cross-linked polyimide membranes induced by different generations of diamino-butane (DAB) dendrimers, J. Membr. Sci. 238 (2004) 153–163.
- [30] Y.C. Xiao, L. Shao, T.S. Chung, D.A. Schiraldi, Effect of thermal treatment and dendrimers chemical structures on the properties of highly surface crosslinked polyimide films, Ind. Eng. Chem. Res. 44 (2005) 3059–3067.
- [31] M.F. Jimenez-Solomon, P. Gorgojo, M. Munoz-Ibanez, A.G. Livingston, Beneath the surface: influence of supports on thin film composite membranes by interfacial polymerization for organic solvent nanofiltration, J. Membr. Sci. 448 (2013) 102–113.
- [32] D.W. Van Krevelen, Properties of Polymers, Elsevier, Netherlands, 1976.
- [33] A.K. Holda, I.F.J. Vankelecom, Integrally skinned PSf-based SRNF-membranes prepared via phase inversion-Part B: Influence of low molecular weight additives, J. Membr. Sci. 450 (2014) 499–511.
- [34] X.Q. Cheng, L. Shao, C.H. Lau, High flux polyethylene glycol based nanofiltration membranes for water environmental remediation, J. Membr. Sci. 476 (2015) 95–104.
- [35] Y. Liu, R. Wang, T.S. Chung, Chemical cross-linking modification of polyimide membranes for gas separation, J. Membr. Sci. 189 (2001) 231–239.
- [36] Y. Sui, X.R. Zeng, X.N. Fang, X.K. Fu, Y. Xiao, L. Chen, M.H. Li, S. Cheng, Syntheses, structure, redox and catalytic epoxidation properties of dioxomolybdenum (VI) complexes with Schiff base ligands derived from tris(hydroxymethyl) amino methane, J. Mol. Catal. A: Chem. 270 (2007) 61–67.
- [37] Z.J. Liu, F.F. Yu, Q. Zhang, Y. Zeng, Y.H. Wang, Preparation and characterization of a novel polyimide liquid crystal vertical alignment layer, Eur. Polym. J. 44 (2008) 2718–2727.
- [38] Y. Meng, H. Wu, Y. Zhang, Z. Wei, A flexible electrode based on a three-dimensional graphene network-supported polyimide for lithium-ion batteries, J. Mater. Chem. A 2 (2014) 10842–10846.
- [39] J.R. Wiegand, Z.P. Smith, Q. Liu, C.T. Patterson, B.D. Freeman, R. Guo, Synthesis and characterization of triptycene-based polyimides with tunable high fractional free volume for gas separation membranes, J. Mater. Chem. A 2 (2014) 13309–13320.
- [40] L. Shao, Y.P. Bai, X. Huang, L.H. Meng, J. Ma, Fabrication and characterization of solution cast MWNTs/PEI nanocomposites, J. Appl. Polym. Sci. 113 (2009) 1879–1886.
- [41] O. Stoilova, M. Ignatova, N. Manolova, T. Godjevargova, D.G. Mita, I. Rashkov,

- Functionalized electrospun mats form styrene-maleic anhydride copolymers for immobilization of acetylcholinesterase, Eur. Polym. J. 46 (2010) 1966–1974.
- [42] N. Kanzaki, K. Onuma, A. Ito, K. Teraoka, T. Tateishi, S. Tsutsumi, Direct growth rate measurement of hydroxyapatite single crystal by moiré phase shift interferometry, J. Phys. Chem. B 102 (1998) 6471–6476.
- [43] C.E. Powell, X.J. Duthie, S.E. Kentish, G.G. Qiao, G.W. Stevens, Reversible diamine cross-linking of polyimide membranes, J. Membr. Sci. 291 (2007) 199–209
- [44] X.Y. Qiao, T.S. Chung, Diamine modification of P84 polyimide membranes for pervaporation dehydration of isopropanol, AICHE J. 52 (2006) 3462–3472.
- [45] T.H. Yong, L.W. Chen, Pore formation mechanism of membranes from phase inversion process, Desalination 103 (1995) 233–247.
- [46] A.K. Holda, I.F.J. Vankelecom, Understanding and guiding the phase inversion process for synthesis of solvent resistant nanofiltration membranes, J. Appl. Polym. Sci. 132 (2015) 42130.
- [47] A.K. Holda, I.F.J. Vankelecom, Integrally skinned PSf-based SRNF-membranes prepared via phase inversion-Part A: influence of high molecular weight additives, J. Membr. Sci. 450 (2014) 512–521.
- [48] C.M. Kee, A. Idris, Permeability performance of different molecular weight cellulose acetate hemodialysis membrane, Sep. Purif. Technol. 75 (2010) 102–113.
- [49] A.L. Gao, F. Liu, H.Y. Shi, L.X. Xue, Controllable transition from finger-like pores to inter-connected pores of PLLA membranes, J. Membr. Sci. 478 (2015) 96–104.
- [50] N. Peng, T.S. Chung, K.Y. Li, The role of additives on dope rheology and membrane formation of defect-free Torlon<sup>®</sup> hollow fiber for gas separation, J. Membr. Sci. 343 (2009) 62–72.
- [51] A. Ananth, G. Arthanareeswaran, H.T. Wang, The influence of tetraethylorthosilicate and polyethyleneimine on the performance of polyethersulfone membranes, Desalination 287 (2012) 61–70.
- [52] Z.G. Wang, Z.K. Xu, L.S. Wan, Modulation the morphologies and performance of polyacrylonitrile-based asymmetric membranes containing reactive groups: effect of non-solvents in the dope solution, J. Membr. Sci. 278 (2006) 447–456.
- [53] Y.H. See-Toh, M. Silva, A.G. Livingston, Controlling molecular weight cut-off curves for highly solvent stable organic solvent nanofiltration (OSN) membranes, J. Membr. Sci. 324 (2008) 220–232.
- [54] M. Aoki, N. Asano, K. Miyatake, H. Uchida, M. Watanabe, Durability of sulfonated polyimide membrane evaluated by long-term polymer electrolyte fuel cell operation, J. Electrochem. Soc. 153 (2006) A1154–A1158.
- [55] Z. Ahmad, J.E. Mark, Polyimide-ceramic hybrid composites by the sol-gel route, Chem. Mater. 13 (2001) 3320–3330.
- [56] J.S. Kang, J. Won, H.C. Park, U.Y. Kim, Y.S. Kang, Y.M. Lee, Morphology control of asymmetric membranes by UV irradiation on polyimide dope solution, J. Membr. Sci. 169 (2000) 229–235.
- [57] A.F.M. Barton, Handbook of Solubility Parameters and Other Cohesion Parameters, 2nd ed., CRC Press, Boca Raton, 1984.
- [58] S.P. Sun, T.S. Chung, Enhancement of flux and solvent stability of Matrimid thin-film composite membranes for organic solvent nanofiltration, AICHE J. 60 (2014) 3623–3633.
- [59] S.P. Sun, S.Y. Chan, T.S. Chung, A slow-fast phase separation (SFPS) process to fabricate dual-layer hollow fiber substrates for thin-film composite (TFC) organic solvent nanofiltration (OSN) membranes, Chem. Eng. Sci. 129 (2015) 232–242.
- [60] X.F. Li, S.D. Feyter, I.F.J. Vankelecom, Poly(sulfone)/sulfonated poly(ether ether ketone) blend membranes: morphology study and application in the filtration of alcohol based feeds, J. Membr. Sci. 324 (2008) 67–75.
- [61] J. Li, M. Wang, Y. Huang, B. Luo, Y. Zhang, Q. Yuan, Separation of binary solvent mixtures with solvent resistant nanofiltration membranes Part A: investigation of separation performance, RSC Adv. 4 (2014) 40740–40747.
- [62] P. Vandezande, X.F. Li, L.E.M. Gevers, I.F.J. Vankelecom, High throughput study of phase inversion parameters for polyimide-based SRNF membranes, J. Membr. Sci. 330 (2009) 307–331.
- [63] S.M. Dutczak, C.R. Tanardi, K.K. Kopeć, M. Wessling, D. Stamatialis, "Chemistry in a spinneret" to fabricate hollow fibers for organic solvent filtration, Sep. Purif. Technol. 86 (2012) 183–189.
- [64] S.M. Dutczak, F.P. Cuperus, M. Wessling, D. Stamatialis, New crosslinking method of polyamide–imide membranes for potential application in harsh polar aprotic solvents, Sep. Purif. Technol. 102 (2013) 142–146.
- [65] V. Discart, M.B. Bilad, R. Moorkens, H. Arafat, I.F.J. Vankelecom, Decreasing membrane fouling during Chlorella vulgaris broth filtration via membrane development and coagulant assisted filtration, Algal Res. 9 (2015) 55–64.
- [66] P. Vandezande, L.E.M. Gevers, P.A. Jacobs, I.F.J. Vankelecom, Preparation parameters influencing the performance of SRNF membranes cast from polyimide solutions via SEPPI, Sep. Purif. Technol. 66 (2009) 104–110.